

Record Antiferromagnetic Coupling for a 3d/4d Cyanide-Bridged Compound

Dawid Pinkowicz,[†] Heather Southerland,[‡] Xin-Yi Wang,[§] and Kim R. Dunbar^{*‡}

[†]Faculty of Chemistry, Jagiellonian University, Ingardena 3, 30-060 Kraków, Poland

[‡]Department of Chemistry, Texas A&M University, College Station, Texas 77842-3012, United States

[§]State Key Laboratory of Coordination Chemistry, School of Chemistry and Chemical Engineering, Nanjing University, Nanjing 210093, China

S Supporting Information

ABSTRACT: The pentanuclear compound $[\text{V}^{\text{II}}(\text{tmphen})_2]_3[\text{Mo}^{\text{III}}(\text{CN})_6]_2$ (tmphen = 3,4,7,8-tetramethyl-1,10-phenanthroline) exhibits a record antiferromagnetic exchange coupling constant of $J_{\text{V-Mo}} = -114 \text{ cm}^{-1}$. This is the first example of a heterobimetallic cyanide compound with such strong magnetic coupling.

Cyanide-based materials^{1–3} have been known since the discovery of Prussian blue by Diesbach in 1704.⁴ After nearly 300 years, an upsurge of interest in cyanide-based Prussian blue analogues (PBAs) occurred, with some examples exhibiting extraordinarily strong magnetic coupling between the metal centers, leading to room temperature magnets.^{5–7} The compound $\text{KV}^{\text{II}}[\text{Cr}^{\text{III}}(\text{CN})_6]$ exhibits the highest long-range magnetic ordering temperature with $T_c = 376 \text{ K}$.^{8,9} In 2005 Ruiz et al.¹⁰ predicted that the use of 4d and 5d cyanometalate building blocks in combination with early 3d transition elements should lead to even stronger coupling for specific combinations of metals in the $\text{M-CN-M}'$ linkage and higher critical temperatures for Prussian blue phases that contain them. For example, the predicted ordering temperature for a hypothetical $\text{Mo}^{\text{III}}\text{-V}^{\text{II}}$ PBA is predicted to be 552 K with an antiferromagnetic coupling constant of $J_{\text{Mo-V}} \approx -400 \text{ cm}^{-1}$.

The enhanced magnetic coupling in cyanide-bridged $\text{M-CN-M}'$ compounds involving heavier transition metals M is attributed to the diffuse nature of their 4d/5d orbitals which can overlap more efficiently with the respective orbitals of the cyanide bridge. The two known homoleptic Mo^{III} cyanometalate anions are $[\text{Mo}^{\text{III}}(\text{CN})_7]^{4-}$ ¹¹ and $[\text{Mo}^{\text{III}}(\text{CN})_6]^{3-}$,¹² and there are two heteroleptic compounds as well.¹³ Importantly, there are only a few examples of well-characterized heterometallic CN-bridged compounds containing these precursors, the majority of the cases involving Mn^{II} .^{13–18} The most interesting compounds vis-à-vis magnetic properties are a trinuclear molecule reported by our groups with Mn^{II} and $[\text{Mo}^{\text{III}}(\text{CN})_7]^{4-}$, which has the highest barrier and hysteresis temperatures among cyanide single-molecule magnets, and two examples of $\text{V}^{\text{II}}\text{-Mo}^{\text{III}}$ assemblies, including a pentanuclear $\text{V}^{\text{II}}_4\text{Mo}^{\text{III}}$ molecule based on $[\text{Mo}^{\text{III}}(\text{CN})_6]^{3-}$ with the strongest antiferromagnetic coupling reported to date for a heterobimetallic CN-bridged species ($J_{\text{Mo-V}} = -61 \text{ cm}^{-1}$)¹⁹ and an amorphous magnet with $T_c = 110 \text{ K}$.²⁰

In this contribution, we present a new member of the family of pentanuclear trigonal-bipyramidal (TBP) cages^{21–25} based on the $\text{Mo}^{\text{III}}\text{-CN-V}^{\text{II}}$ combination,¹⁰ namely, $[\text{V}^{\text{II}}(\text{tmphen})_2]_3[\text{Mo}^{\text{III}}(\text{CN})_6]_2(\text{MeOH})_{12}(\text{MeCN})_2$ (tmphen = 3,4,7,8-tetramethyl-1,10-phenanthroline), which exhibits a new record high for antiferromagnetic coupling ($J_{\text{Mo-V}} = -114 \text{ cm}^{-1}$) by superexchange through the $\text{M-CN-M}'$ linkage.

The design of the new V_3Mo_2 compound (denoted as V_3Mo_2) follows the well-established building block approach to Prussian blue mimics with TBP geometries.²⁶ The use of two 1,10-phenanthroline-type capping ligands with a 3d metal center enforces the formation of a cis complex with two open coordination sites that is well-suited for the self-assembly of a discrete cage with hexacyanometalates (Figure S1 in the Supporting Information).

The new compound (Figure 1 and Figure S2 in the Supporting Information) crystallizes as dark blue needle

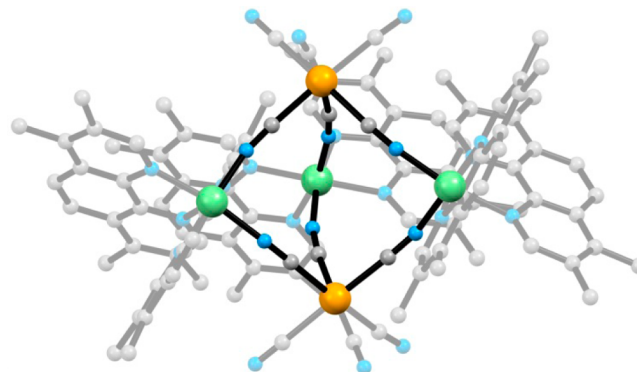


Figure 1. Molecular structure of $[\text{V}^{\text{II}}(\text{tmphen})_2]_3[\text{Mo}^{\text{III}}(\text{CN})_6]_2$. Colors: Mo, orange; V, green; C, gray; N, blue. Hydrogen atoms and solvent molecules have been omitted for the sake of clarity.

crystals (monoclinic, $P2_1/c$)²⁷ that grew from a MeOH/MeCN solution of an in situ-prepared “ $[\text{V}^{\text{II}}(\text{tmphen})_2]^{2+}$ ” precursor and $[\text{Mo}^{\text{III}}(\text{CN})_7]^{4-}$, which loses one of the CN^- ligands during the course of the reaction.^{21,28} The V_3Mo_2 product is a TBP molecule with two $[\text{Mo}^{\text{III}}(\text{CN})_6]^{3-}$ anions in the apical positions acting as facial capping bridges for three

Received: May 8, 2014

Published: June 30, 2014

$[\text{V}^{\text{II}}(\text{tmphen})_2]^{2+}$ units. Each Mo^{III} ion is in a slightly distorted octahedral geometry with Mo–C bond lengths in the range 2.12–2.20 Å, consistent with those reported previously for $[\text{Mo}^{\text{III}}(\text{CN})_6]^{3-}$ compounds.^{12,19,21} The coordination spheres of the V^{II} ions are distorted from octahedral symmetry, with two V– N_{CN} bonds in the range 2.01–2.06 Å and four V– N_{tmphen} bonds that span the distances 2.12–2.16 Å, similar to other V^{II} cyanide¹⁹ and diimine^{29,30} complexes. The $\text{Mo}^{\text{III}}\text{–CN–V}^{\text{II}}$ bridges exhibit Mo–C–N and V–N–C angles in the 170.0–177.3° and 161.6–168.1° ranges, respectively, which are typical.^{19,21} Four of the six tmphen ligands exhibit two intramolecular $\pi\text{–}\pi$ interactions at 3.53 and 3.54 Å. The remaining two tmphen ligands are engaged in intermolecular $\pi\text{–}\pi$ interactions with two ligands of the adjacent TBP complex, resulting in the formation of the supramolecular “dimer” depicted in Figure S3 in the Supporting Information. These four tmphen ligands are arranged in an interdigitated manner with interplanar distances in the 3.49–3.55 Å range. In addition, the entire crystal structure is stabilized by hydrogen bonding involving MeOH and face-to-edge $\pi\text{–}\pi$ interactions.

The magnetic properties of crushed crystals of $[\text{V}^{\text{II}}(\text{tmphen})_2]_3[\text{Mo}^{\text{III}}(\text{CN})_6]_2\cdot(\text{MeOH})_{12}\cdot(\text{MeCN})_2$ were investigated by variable-temperature magnetic susceptibility measurements from 1.8 to 335 K under an applied field of 0.3 T and by magnetization measurements in the 0–7 T magnetic field range at 1.8 K.³¹ The $\chi_{\text{M}}T$ versus T plot (Figure 2) exhibits a steady decrease from a value of 2.11 emu K mol^{-1}

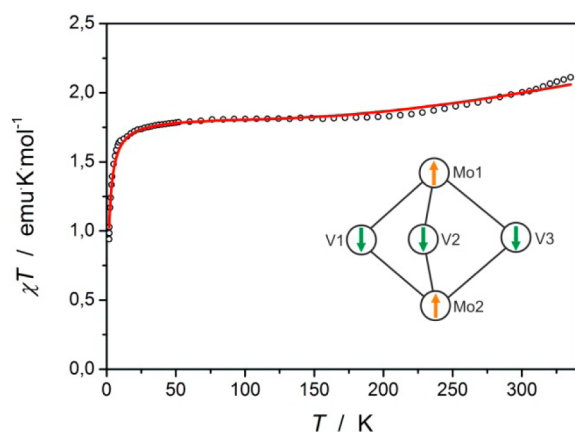


Figure 2. Experimental $\chi_{\text{M}}T$ vs T plot for V_3Mo_2 measured under an applied magnetic field of 0.3 T (circles). The red line corresponds to a fit resulting in an average g factor (g_{av}) of 1.97 for the Mo^{III} and V^{II} centers, an average antiferromagnetic exchange coupling constant ($J_{\text{Mo–V}}$) of -114 cm^{-1} , and an intermolecular exchange constant (zJ') of -0.19 cm^{-1} . Inset: the antiparallel arrangement of the spins of V^{II} and Mo^{III} resulting from strong antiferromagnetic coupling.

at 335 K, which is well below the spin-only value of 9.375 emu K mol^{-1} expected for five uncoupled $S = 3/2$ metal centers (three $S_{\text{V}} = 3/2$ and two $S_{\text{Mo}} = 3/2$), to a plateau in the 200–50 K range at a value of 1.81 emu K mol^{-1} , which is very close to the value of 1.875 emu K mol^{-1} expected for an $S = 3/2$ ground state (five antiferromagnetically coupled $S = 3/2$ metal centers; Figure 2 inset). Such behavior indicates unusually strong antiferromagnetic coupling between the Mo^{III} and V^{II} spin centers as predicted by Ruiz et al.¹⁰ Any attempt to extend the measurement range above 335 K led to decomposition of the sample, as judged by an abrupt drop of the magnetic moment, which is consistent with the results of the thermogravimetric

analysis (TGA) (Figure S4 in the Supporting Information). The $\chi_{\text{M}}T$ versus T plot was fit over the accessible temperature range using the PHI software program (version 2.0, approximation mode) and the following Hamiltonian:

$$\hat{H} = -2J_{\text{Mo–V}}(\hat{S}_{\text{Mo1}} + \hat{S}_{\text{Mo2}})(\hat{S}_{\text{V1}} + \hat{S}_{\text{V2}} + \hat{S}_{\text{V3}}) + \mu_{\text{B}}Hg_{\text{av}}(\hat{S}_{\text{Mo1}} + \hat{S}_{\text{Mo2}} + \hat{S}_{\text{V1}} + \hat{S}_{\text{V2}} + \hat{S}_{\text{V3}}) \quad (\text{eq 1})$$

where only $J_{\text{Mo–V}}$ and g_{av} were allowed to vary. The intermolecular interactions zJ' were introduced into the best fit by using the mean-field approximation:

$$\chi_{\text{mean}} = \frac{\chi_{\text{fit}}}{1 - \frac{2zJ'}{Ng^2\mu_{\text{B}}}\chi_{\text{fit}}} \quad (\text{eq 2})$$

The fitting procedure led to the values $J_{\text{Mo–V}} = -114 \text{ cm}^{-1}$, $g_{\text{av}} = 1.97$, and $zJ' = -0.19 \text{ cm}^{-1}$. The decrease in the $\chi_{\text{M}}T$ product at low temperatures below 10 K is most likely due to intermolecular antiferromagnetic interactions, as anticipated from the sign of the mean-field parameter zJ' , but may also reflect zero-field splitting and spin–orbit coupling effects.³²

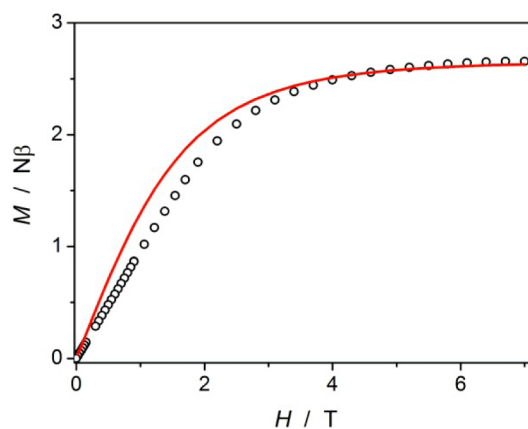


Figure 3. Plot of M vs H for V_3Mo_2 measured at 1.8 K (circles). The red line corresponds to a simulation for three $S = 3/2$ V^{II} centers antiferromagnetically coupled with two $S = 3/2$ Mo^{III} centers assuming $g_{\text{av}} = 1.81$ and $J_{\text{Mo–V}} = -114 \text{ cm}^{-1}$.

The dependence of M on H (Figure 3) is typical for an $S = 3/2$ paramagnet, *viz.*, it increases linearly up to 2 T and then slowly saturates, approaching $2.7N\beta$ at $H = 7$ T, which is close to the expected spin-only value of $3.0N\beta$ for an $S = 3/2$ ground state resulting from five antiferromagnetically coupled $S = 3/2$ metal centers. A simulation of the $M(H)$ dependence (red line in Figure 3) assuming $J_{\text{Mo–V}} = -114 \text{ cm}^{-1}$ and $g_{\text{av}} = 1.81$ corresponds well with the experimental data, which corroborates the anticipated $S = 3/2$ ground state and strong antiferromagnetic coupling for the $\text{Mo}^{\text{III}}\text{–CN–V}^{\text{II}}$ spin pairs. There is no evidence for slow paramagnetic relaxation, as judged by the fact that there is no out-of-phase signal and no frequency dependence for the in-phase AC magnetic susceptibility.

In summary, a pentanuclear $\text{V}_3^{\text{II}}\text{Mo}_2^{\text{III}}$ compound based on the 4d cyanometalate $[\text{Mo}^{\text{III}}(\text{CN})_6]^{3-}$ and the early 3d transition-metal capping group $[\text{V}^{\text{II}}(\text{tmphen})_2]^{2+}$ has been prepared. The magnetic properties of the trigonal-bipyramidal molecule $[\text{V}^{\text{II}}(\text{tmphen})_2]_3[\text{Mo}^{\text{III}}(\text{CN})_6]_2\cdot(\text{MeOH})_{12}\cdot(\text{MeCN})_2$

reveal extremely strong antiferromagnetic interactions between the cyanide-bridged Mo^{III} and V^{II} metal centers, with a coupling constant estimated to be -114 cm^{-1} , which is the strongest magnetic coupling ever reported for a heterobimetallic cyanide compound.

■ ASSOCIATED CONTENT

■ Supporting Information

Additional structural diagrams, TGA plots, description of alternate attempts to fit the magnetic data, PXRD results, and a crystallographic information file. This material is available free of charge via the Internet at <http://pubs.acs.org>. The crystallographic data have also been deposited at the Cambridge Crystallographic Data Centre under deposition number CCDC 994436 and are available via www.ccdc.cam.ac.uk/data_request/cif.

■ AUTHOR INFORMATION

Corresponding Author

dunbar@chem.tamu.edu

Notes

The authors declare no competing financial interest.

■ ACKNOWLEDGMENTS

K.R.D. thanks the Department of Energy (DE-FG02-02ER45999) for financial support. D.P. gratefully acknowledges the financial support of the European Commission within the Marie Curie International Outgoing Fellowship, Project MultiCyChem (Grant Agreement PEOF-GA-2011-298569), and the START Fellowship of the Foundation for Polish Science (2013 edition).

■ REFERENCES

- (1) Shatruk, M.; Avendano, C.; Dunbar, K. R. *Prog. Inorg. Chem.* **2009**, *56*, 155–334.
- (2) Verdager, M.; Girolami, G. S. *Magnetic Prussian Blue Analogs. In Magnetism: Molecules to Materials V*; Wiley-VCH: Weinheim, Germany, 2005; pp 283–346.
- (3) Nowicka, B.; Korzeniak, T.; Stefańczyk, O.; Pinkowicz, D.; Chorąży, S.; Podgajny, R.; Sieklucka, B. *Coord. Chem. Rev.* **2012**, *256*, 1946–1971.
- (4) Anonymous. *Miscnea Berol. Soc. Sci.* **1710**, *1*, 377–378.
- (5) Mallah, T.; Thiébaud, S.; Verdager, M.; Veillet, P. *Science* **1993**, *262*, 1554–1557.
- (6) Ferlay, S.; Mallah, T.; Ouahes, R.; Veillet, P.; Verdager, M. *Nature* **1995**, *378*, 701–703.
- (7) Hatlevik, Ø.; Buschmann, W. E.; Zhang, J.; Manson, J. L.; Miller, J. S. *Adv. Mater.* **1999**, *11*, 914–918.
- (8) Holmes, S. M. Ph.D. Thesis, University of Illinois at Urbana-Champaign, Champaign, IL, 2000.
- (9) Holmes, S. M.; Girolami, G. S. *J. Am. Chem. Soc.* **1999**, *121*, 5593–5594.
- (10) Ruiz, E.; Rodríguez-Forste, A.; Alvarez, S.; Verdager, M. *Chem.—Eur. J.* **2005**, *11*, 2135–2144.
- (11) Young, R. C. *J. Am. Chem. Soc.* **1932**, *54*, 1402–1405.
- (12) Beauvais, L. G.; Long, J. R. *J. Am. Chem. Soc.* **2002**, *124*, 2110–2111.
- (13) Shores, M. P.; Sokol, J. J.; Long, J. R. *J. Am. Chem. Soc.* **2002**, *124*, 2279–2292.
- (14) Larionova, J.; Clérac, R.; Sanchiz, J.; Kahn, O.; Golhen, S.; Ouahab, L. *J. Am. Chem. Soc.* **1998**, *120*, 13088–13095.
- (15) Kahn, O.; Larionova, J.; Ouahab, L. *Chem. Commun.* **1999**, 945–952.
- (16) Larionova, J.; Kahn, O.; Golhen, S.; Ouahab, L.; Clérac, R. *Inorg. Chem.* **1999**, *38*, 3621–3627.
- (17) Milon, J.; Guionneau, P.; Duhayon, C.; Sutter, J.-P. *New J. Chem.* **2011**, *35*, 1211–1218.
- (18) Wang, Q.-L.; Southerland, H.; Li, J.-R.; Prosvirin, A. V.; Zhao, H.; Dunbar, K. R. *Angew. Chem., Int. Ed.* **2012**, *51*, 9321–9324.
- (19) Freedman, D. E.; Jenkins, D. M.; Long, J. R. *Chem. Commun.* **2009**, 4829–4831.
- (20) Tomono, K.; Tsunobuchi, Y.; Nakabayashi, K.; Ohkoshi, S. I. *Inorg. Chem.* **2010**, *49*, 1298–1300.
- (21) Wang, X.-Y.; Hilfiger, M. G.; Prosvirin, A.; Dunbar, K. R. *Chem. Commun.* **2010**, 46, 4484–4486.
- (22) Hilfiger, M. G.; Shatruk, M.; Prosvirin, A.; Dunbar, K. R. *Chem. Commun.* **2008**, 5752–5754.
- (23) Funck, K. E.; Hilfiger, M. G.; Berlinguette, C. P.; Shatruk, M.; Wernsdorfer, W.; Dunbar, K. R. *Inorg. Chem.* **2009**, *48*, 3438–3452.
- (24) Hilfiger, M. G.; Chen, M.; Brinzari, T. V.; Nocera, T. M.; Shatruk, M.; Petasis, D. T.; Musfeldt, J. L.; Achim, C.; Dunbar, K. R. *Angew. Chem., Int. Ed.* **2010**, *49*, 1410–1413.
- (25) Funck, K. E.; Prosvirin, A. V.; Mathonière, C.; Clérac, R.; Dunbar, K. R. *Inorg. Chem.* **2011**, *50*, 2782–2789.
- (26) Shatruk, M.; Chambers, K. E.; Prosvirin, A. V.; Dunbar, K. R. *Inorg. Chem.* **2007**, *46*, 5155–5165.
- (27) Crystallographic parameters for V_3Mo_2 : $C_{124}H_{96}Mo_2N_{26}O_{12}V_3$, monoclinic, $P2_1/c$, $a = 19.550(3)\text{ \AA}$, $b = 25.687(4)\text{ \AA}$, $c = 24.744(4)\text{ \AA}$, $\beta = 98.171(2)^\circ$, $V = 12\,300(3)\text{ \AA}^3$, $Z = 4$, $\mu = 0.487\text{ mm}^{-1}$, $T = 110(1)\text{ K}$, Mo $K\alpha$ radiation ($\lambda = 0.71073\text{ \AA}$), $R_1 = 0.0979$ for 1504 parameters and 10 307 unique reflections with $I > 2\sigma(I)$, $wR_2 = 0.3480$ for all 21 612 reflections, GOF = 1.196, data completeness 0.997.
- (28) All manipulations were performed under an inert atmosphere. Solvents were deoxygenated prior to use by distillation under N_2 . Preparation of V_3Mo_2 : $V^{II}(\text{MeCN})_6(\text{BPh}_4)_2$ (1.12 g, 1.2 mmol) and tmphen (0.570 g, 2.4 mmol) were dissolved in a mixture of MeOH (16.4 mL) and MeCN (30.5 mL) to form a dark-blue solution that was layered on a greenish-yellow solution of $K_3[\text{Mo}^{III}(\text{CN})_6] \cdot 2H_2O$ (1.410 g, 3.0 mmol) and 18-crown-6 ether (3.168 g, 12.0 mmol) in MeOH (38 mL). The layering was performed in nine 20 mL vials (3 cm in diameter). After 1 day, the two layers had mixed completely to give a homogeneous dark-blue solution; 3 days later (5–8), dark-blue needle crystals had formed. The product was separated by repeated decanting with subsequent washing with MeCN and stored under MeCN. Yield: 110 mg (11%). Elemental analysis (EA) calcd for $[V^{II}(\text{tmphen})_2]_3[\text{Mo}^{III}(\text{CN})_6]_2 \cdot (\text{MeOH})_{12} \cdot (\text{MeCN})_2$ (%): C, 58.60; H, 5.95; N, 14.33; O, 7.55. Found: C, 58.26; H, 4.81; N, 14.63; O, 6.16. The discrepancy in the EA arises from the fact that V_3Mo_2 rapidly loses solvent molecules (see the TGA curve in Figure S4 in the Supporting Information) and exchanges them with water. An improved match was obtained for the formula $[V^{II}(\text{tmphen})_2]_3[\text{Mo}^{III}(\text{CN})_6]_2 \cdot (\text{MeOH})_5 \cdot (\text{MeCN}) \cdot (H_2O)_5$: C, 58.38; H, 5.50; N, 14.80; O, 6.76. The purity of the compound was checked by performing powder X-ray diffraction (PXRD) in a glass capillary under solvent using a single-crystal X-ray diffractometer (Figure S5 in the Supporting Information).
- (29) Vinklárček, J.; Hurýchová, H.; Honzíček, J.; Šebestová, L.; Padělková, Z.; Řezáčová, M. *Eur. J. Inorg. Chem.* **2013**, 2665–2672.
- (30) Cotton, F. A.; Falvello, L. R.; Llusar, R.; Libby, E.; Murillo, C. A.; Schwotzer, W. *Inorg. Chem.* **1986**, *25*, 3423–3428.
- (31) Magnetic measurements were performed on six different batches of V_3Mo_2 with the sample immersed in acetonitrile to prevent solvent loss during the measurements. Samples were measured in a sealed NMR tube and a Delrin sample holder developed in the Dunbar group. The results presented herein are from the measurements using the Delrin holder. Magnetic data were corrected for the diamagnetism of the holder, the diamagnetic contribution of the MeCN solvent, and the diamagnetism of the compound (Pascal constants).
- (32) Detailed versions of alternative attempts to fit the magnetic data are included in the Supporting Information.